

# Filtering $h_{int}$ Images for the Detection of Microcalcifications

Marius George Linguraru, Michael Brady, and Margaret Yam

University of Oxford, Medical Vision Laboratory,  
Old Library, Parks Road, Oxford OX1 3PJ, UK  
mglin@robots.ox.ac.uk

**Abstract.** Recent figures show that approximately 1 in 11 women in the western world will develop breast cancer during the course of their lives. Early detection greatly improves prognosis and considerable research has been undertaken to this end. Mammographic images are difficult to interpret even by radiologists and this makes their task error prone. One of the earliest non-palpable signs is the appearance of microcalcifications, typically 0.5 mm in diameter, representing small deposits of calcium salts in the breast. A novel approach to detecting microcalcifications in x-ray mammography has been explored. The method is based on the use of the physics-based image representation  $h_{int}$  [1] and use of anisotropic diffusion to filter  $h_{int}$  images. The diffusion process becomes a method of detecting both noise and microcalcifications in mammograms.

## 1 Theory

The  $h_{int}$  representation results from a model of the mammogram image formation process. The appearance of mammograms varies massively according to the specific conditions, though the object of interest, the breast anatomy, remains invariant. The  $h_{int}$  model offers an alternative quantitative representation of the breast tissue, where the  $h_{int}$  of a pixel represents the amount of non-fatty breast tissue at that point. Figure 1.a shows a depiction of the  $h_{int}$  surface of a breast. An  $h_{int}$  representation can be easily visualised as an image, since the  $h_{int}$  values are in float format, where brighter parts correspond to regions of the breast with more interesting (non-fatty) tissue or calcifications, as shown in Figure 1.b. While microcalcifications appear in about 14% of mammograms, they are typically small and sparse. For this reason, Highnam and Brady's algorithm for estimating  $h_{int}$  [1] assumes only two types of tissue: fat and non-fat (i.e. parenchymal, tumour). Since the attenuation coefficient of microcalcification is typically 26 times that of *interesting tissue*, microcalcifications appear in  $h_{int}$  images as tall thin towers, Figure 2.a.

One of the major characteristics that we use in detecting microcalcifications is the difference that should be visible in the shape of a microcalcification versus noise [1]. While microcalcifications are anatomical structures with slightly blurred edges which appear in mammograms due to the effect of x-ray beams passing through the breast anatomical structure, noise tends to have extremely

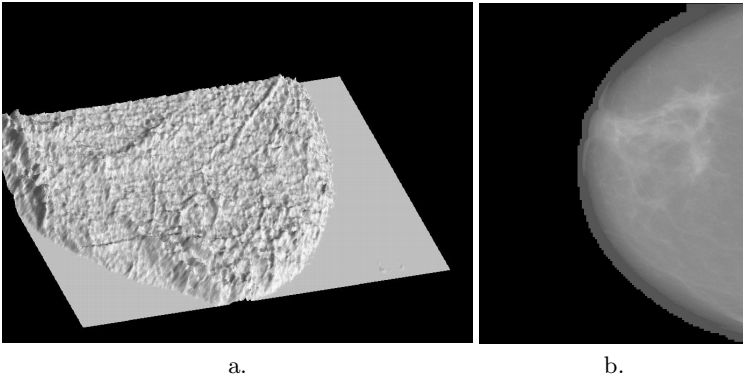


**Fig. 1.** (a) A depiction of the  $h_{int}$  surface of a breast, (b) an  $h_{int}$  representation visualised as an image.

sharp edges, as shown in Figure 2.b. Shot-noise may drastically influence the local image characteristics and represents the main source of false positives (FPs) in algorithms for microcalcification detection. We have previously demonstrated that the  $h_{int}$  representation can eradicate this type of noise [2], but since our method aims to detect shot noise as well, we did not remove shot noise from the images we tested. The appearance of  $h_{int}$  images would be extremely noisy, mainly due to the removal of the glare effect [2], extra-focal and scattered radiation [1] (which accounts for up to 40% of the total radiation exiting the breast). This would make the examination of the regions of interest difficult, making it harder to distinguish small structures in mammograms. Since microcalcifications correspond to high peaks in  $h_{int}$  images, only the most prominent spots of noise may lead towards FPs, the smaller ones being easily removed by the diffusion process. If glare is removed, facilitating the elimination of shot noise, the price to be paid is a massive decrease in the signal to noise ratio (SNR) in  $h_{int}$  [5]. Yam [6] attempts to overcome this visible increase in noise by Wiener filtering the original image before generating  $h_{int}$  surfaces, an approach that improves slightly the SNR. We prefer to work with the glare de-convolved (no shot noise removed) image and use anisotropic diffusion to differentiate edge sharpness of noise and microcalcifications.

## 2 Filter Model

We choose an anisotropic diffusion-based filter [3], [4] which aims to blur the input mammographic image while preserving some small regions of interest. The process relies on the use of a set of different parameters, e.g. time, contrast, size, and it is essential to determine the right choice of parameters. Figure 3 shows different output images after using anisotropic diffusion on a grey-level digital mammogram containing both a calcification and a large spot of noise.

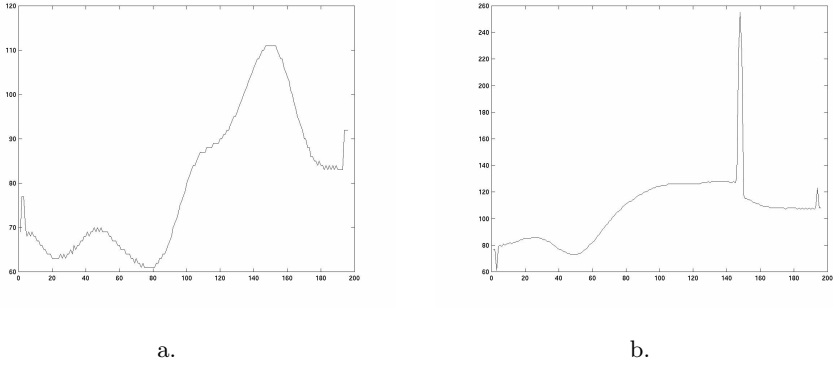


**Fig. 2.** (a) The plot of a filtered intensity image containing a microcalcification at position 150, (b) the plot of a filtered intensity image containing noise at position 147.

We found that Weickert’s solution [4] for the diffusion tensor is best suited to our problem. We used a similar simplified tensor having eigenvalues (1), (2):

$$\lambda_1 = \begin{cases} 1 & |\nabla u_\sigma| = 0, \\ 1 - \exp\left(\frac{-1}{(|\nabla u_\sigma|/\lambda)^s}\right) & |\nabla u_\sigma| > 0 \end{cases} \quad (1)$$

$$\lambda_2 = 1. \quad (2)$$

Nonlinear anisotropic filtering proves to be highly flexible due to the variability of its parameters which help in covering a rather extensive set of possibilities in multi-scaling filtering with respect to the output one can get by filtering medical images, as Table 1 shows.

**Table 1.** Variation of anisotropic diffusion parameters:  $k$  - the contrast factor,  $\sigma$  - the scaling factor and  $t$  - the number of iterations;  $\nearrow$  represents an increase, while  $\searrow$  is a decrease of the parameter or feature.

	Blur in Image	Anatomical Features	Edges
$k \nearrow$	$\nearrow$	$\searrow$	$\searrow \searrow$
$\sigma \nearrow$	$\nearrow$	$\searrow$	$\searrow$
$t \nearrow$	$\nearrow$	$\searrow \searrow$	well preserved over a long time

Having obtained the anisotropically diffused image, we subtract it from the less blurred original. Some differences in the way microcalcifications, as opposed to noise, are diffused can be seen in Figure 4. Microcalcifications tend to be

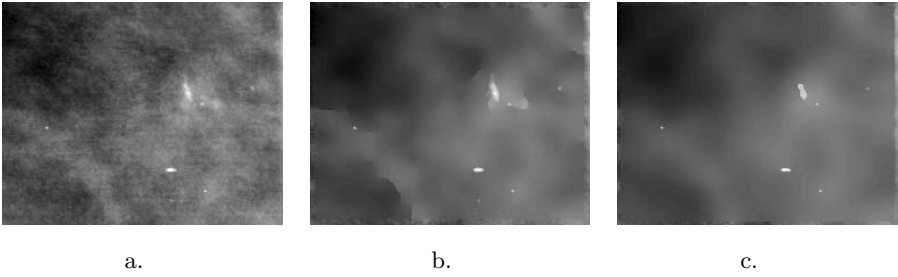


**Fig. 3.** (a) The original 533x386 grey-level image containing a microcalcification in the centre-right of the image and a large spot of noise on the lower side of the image; (b) the diffused image with  $k = 5, \sigma = 0.6$  and  $t = 20$ ; (c) the diffused image with  $k = 5, \sigma = 0.5$  and  $t = 40$ , where only the important small structures are kept and their edges enhanced.

smoothed faster than prominent noise spots, for an appropriate choice of parameters. After a certain number of iterations, the surface of the difference image contains significant changes for noise only.

### 3 Results

We first show some results of applying nonlinear anisotropic diffusion filtering to samples of real mammograms containing microcalcifications. We de-noise  $h_{int}$  images while preserving only calcifications and significant noise, Figure 5.a, .b, .e, .f.

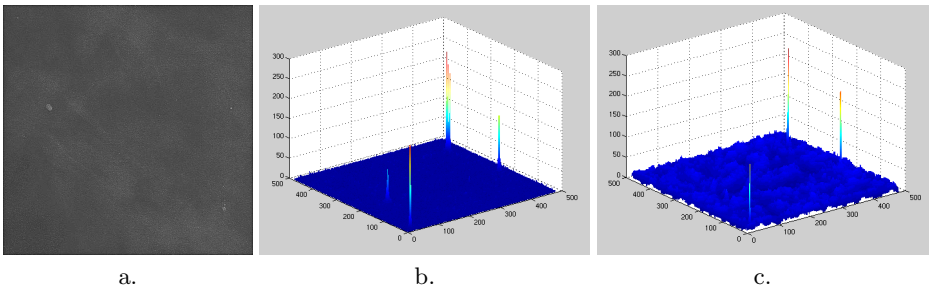


**Fig. 4.** (a) The original preprocessed  $h_{int}$  500x500 image containing a microcalcification on the left side, a large spot of noise on the lower right side and several other smaller noise structures; (b) the 3D plot of the difference image between the original image diffused with  $k = 15, \sigma = 0.6$  and  $t = 5$  and the same one diffused with  $k = 15, \sigma = 0.6$  and  $t = 10$ ; (c) the 3D plot of the difference image between the original image diffused with  $k = 15, \sigma = 0.6$  and  $t = 10$  and the same one diffused with  $k = 15, \sigma = 0.6$  and  $t = 15$ .

In order to reduce processing time and the intervention of the operator in the filtering process, we chose a large value for the contrast factor  $k$ . We still chose a rather small value for the scaling factor  $\sigma$  for preserving tiny anatomical structures or noise over the first iterations in the process of diffusion. Due to the strong variability that exists in mammographic images (e.g. contrast, size of interesting tissue) a multi-scale approach would be preferable. Since the whole process should be robust and easy to use, we reduced the number of variable parameters to one, keeping constant the contrast and scale factors and varying only the number of iterations over a small range. We found that the time factor  $t$  gives optimal results for the filtering process over the whole set of  $h_{int}$  images when we used values between 3 and 7 iterations.

In demonstrating the efficiency of our method in increasing the number of true positives (TPs) we also considered images with high likelihood to present false positives. Such an example is presented in Figure 5.c, .d, .g, .h.

The detection method, of both calcifications and noise was based initially on the association one can make between the original  $h_{int}$  mammograms containing the structures of interest and the surface we built from the filtered images after just a few iterations. Since radiologists may have doubts when searching the original image for microcalcifications, the surface we present would show either hill-shaped structures for microcalcifications or sharp-edged formations for noise in the locations corresponding to the structures of interest. Moreover, we found the simple visual comparison of the two  $h_{int}$  images – the original noisy one and the filtered one – to be quite reliable in differentiating between microcalcifications and noise. While noisy structures tend to be better preserved by the filtering method applied with our final specific choice of parameters, microcalcifications fade faster and look like imploding structures.

### 3.1 Coarse Calcifications

The algorithm was initially tested on a set of 13 samples of average 32-float  $h_{int}$  mammograms containing 10 coarse calcifications pre-labeled by a radiologist and several artifacts. The size of the images varied between 124x180 and 251x251 at 50  $\mu\text{m}$  resolution. The algorithm applied to the enhanced images gave a detection rate of 100%. No FPs were detected during our experiments. The free-response receiver operating characteristic (FROC) curve is shown in Figure 6.a.

### 3.2 Microcalcifications

The algorithm was then further tested on 20 samples of 32-float  $h_{int}$  mammograms containing 27 isolated microcalcifications pre-labeled by a radiologist and various pixels of noise. The size of the samples was 200x250 at a resolution of 50  $\mu\text{m}$ . The set was meant to offer an overview of possible clinical aspects related to microcalcifications of different sizes, some of them clear while some other feint. The TPs fraction was 92.6 % for a number of 0.1 FPs per image.

We further applied an implementation of Yam *et al.*'s algorithm [5] to the same set of microcalcifications. The process differed slightly in this case. The

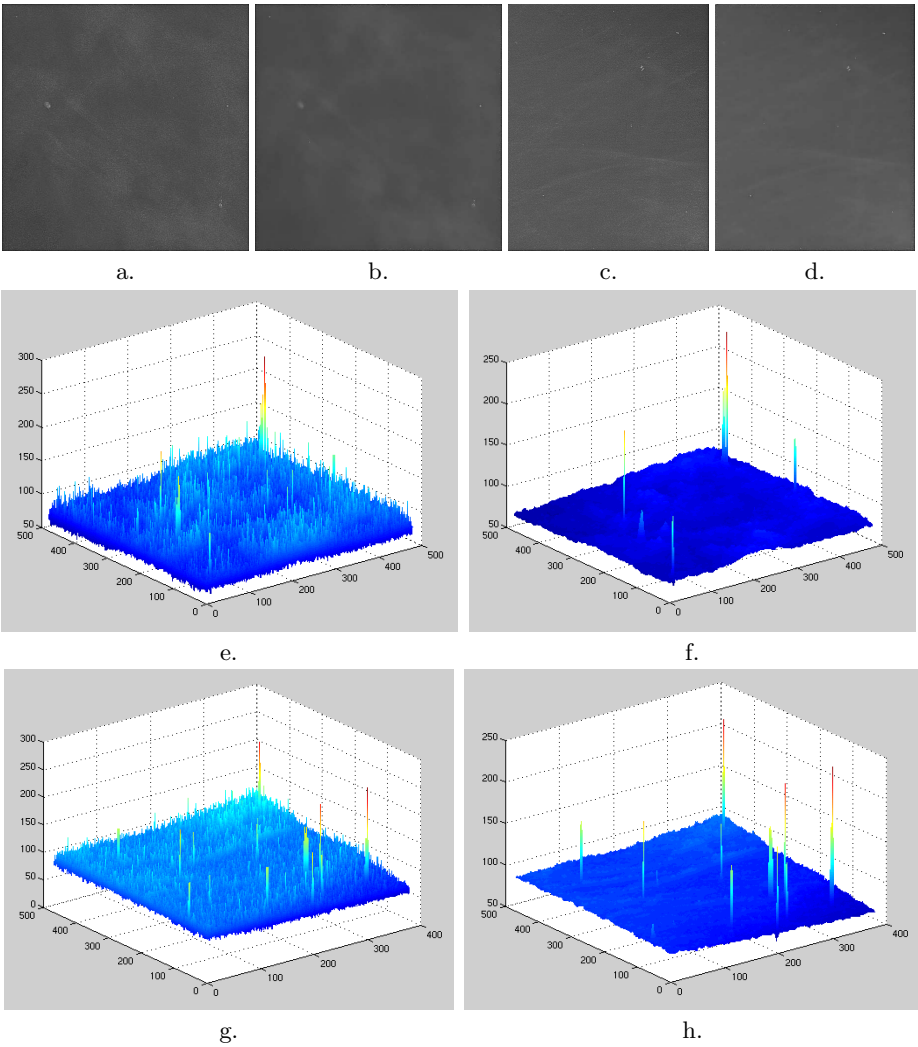


**Fig. 5.** (a) An original preprocessed  $h_{int}$  500x500 image containing a microcalcification on the left side and a large spot of noise on the lower right side; (b) the diffused image from (a) with  $k = 15, \sigma = 0.6$  and  $t = 5$ , we notice that the microcalcification has almost faded, while the noise is still preserved with high contrast; (c) an original preprocessed  $h_{int}$  400x490 image containing only noise structures, the largest piece of noise on the upper right side could be easily considered of being a microcalcification since it does not present very high contrast from the surrounding tissue; (d) the diffused image from (c) with  $k = 15, \sigma = 0.6$  and  $t = 3$ ; (e) the 3D plot of the original  $h_{int}$  image in (a), we notice the extremely noisy appearance where the important structures can be hardly distinguished; (f) the surface of the diffused  $h_{int}$  image in (b), the microcalcification appears as a hill with smoother edges than those of the very sharp-edged noise structures in the same image; (g) the surface of the original  $h_{int}$  image in (c) with highly noisy appearance; (h) the surface of the diffused  $h_{int}$  image in (d) where all structures have very sharp edges and are labeled as noise.

original 32-float  $h_{int}$  mammograms were translated into *tif* images without contrast enhancement, in order to preserve a fixed scale for all mammogram samples. The algorithm developed by Yam *et al.* [5] was applied to the filtered versions of the original images. We obtained a 100% fraction of TPs with a number of 0.3 FPs per image. The FROC curve of the detection using the combination of the anisotropic diffusion filter and the algorithm implemented by Yam *et al.* is shown in Figure 6.b.

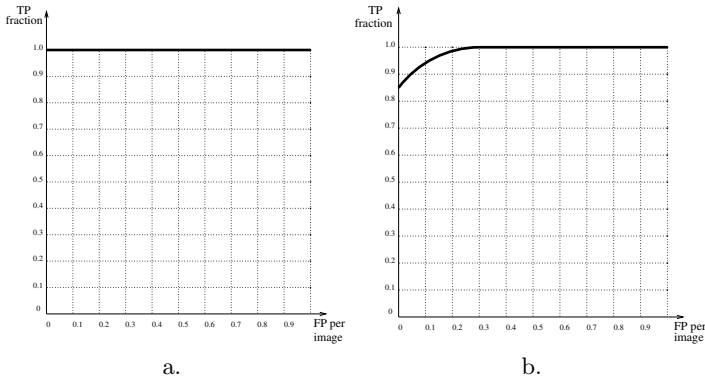


**Fig. 6.** (a) The FROC curve of the detection method for the set of 13 samples containing coarse calcifications; (b) the FROC curve of the combined detection method for the set of 20 samples containing different types of microcalcifications

## 4 Discussion

An important issue in the use of this new filtering method in x-ray mammography is the preservation of tiny anatomical structures over the diffusion process. Unlike most filters which actually blur the whole image and blend small regions together, our method preserves the anatomical independence of all small structures encountered in an image.

A major source of FPs in mammography corresponds to shot noise. The noise maps obtained after removing the glare-effect in the process of generating  $h_{int}$  images can be used as a further step to exclude this specific type of noise from mammograms and therefore reduce the number of FPs. We would therefore expect significantly improved results in the detection process presented in Section 3. As Yam *et al.*'s algorithm is built to use a combination of grey-level and  $h_{int}$  images, using its original implementation on  $h_{int}$ s only is expected to give poorer results. We believe that some changes in the algorithm, such as introducing a threshold that would remove shot noise or any other relevant bits of noise by means of detecting the small area change over the height of the structure, would eliminate most of the detected FPs and would not need to make use of the shot noise maps.

Time is important in the development of real-time clinical applications and filtering algorithms make use of a lot of it because of the subsequent application of kernels over one image. In order to reduce the necessary time for the diffusion process, we used a higher value for the contrast factor  $k$ . A higher  $k$  leads to faster diffusion over the image and fewer iterations are requested. The consistence of our choice is based on the high  $h_{int}$  values corresponding to both shot noise and calcifications. Both structures are preserving their characteristics for high contrast over a few number of iterations.

## 5 Conclusion

We have presented a filtering method based on anisotropic diffusion, a process known for its scale-space and edge detection properties. Our method implements such nonlinear diffusion filtering for the first time in digital mammography and aims to be an alternative to the Wiener filter used previously on breast images.

Our method uses the normalised representation of mammograms that the  $h_{int}$  generation provides, namely a robust and consistent physical-based approach to digital mammography. The initial results are encouraging and further improvements to the method promise better rates of detection. The algorithm is also reliable in detecting both calcifications and noise in a single step by taking into account the *physical* appearance of different structures of interest. While the term noise refers to shot noise only, as the main source of false positives, the term calcifications would include coarse calcifications as well as microcalcifications. Quantum mottle, an important source of errors in mammography, has little interference in our application as it is smoothed by our filter, with a right choice of the contrast and scaling factors. Furthermore, anisotropic diffusion is blurring the images in a more intelligent way than other more usual smoothing filters, making use of the edge enhancement property.

## References

1. Highnam, R. Brady, J.M.: Mammographic Image Analysis. Kluwer Academic Publisher (1999)
2. Highnam, R. Brady, J.M., English, R.: Detecting Film-Screen Artifacts in Mammography using a Model-Based Approach. IEEE Transactions on Medical Imaging **18** (1999) 1016–1024
3. Perona, P. Malik, J.: Scale-space and Edge Detection using Anisotropic Diffusion. IEEE Transactions on Pattern Analysis and Machine Intelligence **12** (1990) 629–639
4. Weickert, J.: A Review of Nonlinear Diffusion Filtering. In: ter Haar Romeny, B. Florack, L. Koenderink, J. Viergever, M. (eds.): Scale-Space Theory in Computer Vision, Lecture Notes in Computer Science, Vol. 1252. Springer, Berlin (1997) 3–28
5. Yam, M. Brady, J.M. Highnam, R. English, R.: De-noising  $h_{int}$  Surfaces: a Physics-based Approach. In: Proc. Medical Image Computing and Computer-Assisted Intervention. Springer (1999) 227-234
6. Yam, M. Highnam, R. Brady, J.M.: Detecting Calcifications using the  $h_{int}$  Representation. In: Computer Assisted Radiology and Surgery. Elsevier (1999) 373-377